Jestr

Research Article

The Compact Slotted Pentaband Inset-Fed Microstrip Patch Antenna for Wireless Applications

Parimal Tiwari[1,*], K K Verma[1] and Chandan[2]

[1]Department of Physics and Electronics, Dr. Rammanohar Lohia Avadh University, Ayodhya, U.P., India.
[2]Department of Electronics and Communication Engineering, Institute of Engineering & Technology, Dr. Rammanohar Lohia Avadh University, Ayodhya, U.P., India.

_____

Abstract

This letter presents a compact slotted pentaband inset-fed microstrip antenna designed to operate for UMTS, WLAN, WiMAX, C-band and X-band applications. By incorporating equispaced slots of same width and length and also the inset feeding, the antenna generates five bands, allowing for penta-band operation. The antenna is manufactured on an FR4 substrate and is excited by an SMA connector using a microstrip line. With its compact dimensions of 25x25x1.6 mm3, the antenna offers a simple structure. Based on the simulated and measured outcomes, the proposed antenna demonstrates numerous advantages, making it highly suitable for wireless communication systems. These advantages include its ability to operate in multiple bands, its percentage bandwidth, compact size, stable radiation pattern, ease of processing, and cost-effectiveness.

Keywords: Inset-fed, UMTS, WLAN, WiMAX, SMA.

_____

1. Introduction

Wireless communication relies on the transmission and reception of electromagnetic waves. The physical layer of communication systems faces significant challenges in terms of bandwidth and interoperability. Meeting the increasing demand for antennas with wide bandwidth, compact size, and low cost has become crucial [1]. Additionally, there is a growing need to develop antennas that can operate in multiple frequency bands, providing advanced functionality compared to other antennas. Achieving multiband capability can be accomplished through various methodologies, such as implementing defected ground structures (DGS) [2,3], split ring resonator (SRR) [4-7] geometries, reconfigurable antennas, implementation of slot structures like meander-shaped and employing different feeding methods [8], or by using the techniques to develop the higher-order modes [9]. Patch antennas are widely used due to their ability to operate across a range of frequencies. Extensive research and various techniques have been developed to achieve the multiple bands and bandwidth for these antennas to operate in the wireless communication.

With number of different sizes, shapes or geometries to design a multiband patch antenna, there comes a numerous types of feeding techniques in which inset feeding is one of such techniques. In this literature several researches with inset feeding and slotted structures have been discussed which can operate in multiband such as S-band, WLAN, WiMAX, C-band X-band, etc. In [10], a microstrip patch antenna with an inset feed has been developed, and its resonant frequency's dependence on the notch gap and feed line geometry has been investigated. The research indicates that a narrower notch gap leads to improved impedance matching. Furthermore, a design rule is established and the performance evaluation of

the proposed design is also presented. In [11], the rectangular patch antenna has been reported which works at a resonant frequency of 2.4 GHz and the inset feeding technique is used. This antenna has the total dimension of patch as 32.5 x 42.1 mm^2 which is much larger than the proposed antenna's substrate dimensions. A reconfigurable E-shaped antenna for dual-band frequency operation is discussed in [12], which is capable of simultaneously switching both the bands without introducing any external network. This antenna has got the dimensions of 50 x 53.5 x 1.55 mm^3 designed using TMM4 substrate. The measured gains are 4.6 dBi, 5.2 dBi, 4.0 dBi, and 4.4 dBi. This antenna is suitable for operating for S-, C- and X-bands, i.e., WiMAX applications, microwave communications and satellite links. [13] presents the design of a rectangular microstrip patch antenna with an inset feed, specifically tailored for wireless applications. The study focuses on investigating the impact of the feeding position on various antenna parameters, such as directivity, gain, return loss, bandwidth, and axial ratio. The patch dimensions itself is having large values as compared to that of the prototype since the width of the patch in this paper is 49.41 mm. The gain and the bandwidth of the design are also varying as the feeding positions are varied. A microstrip antenna having rectangular patch designed and studied for 2.5 GHz ISM band is presented in [14]. Multiple circular slots are introduced on the patch to improve the performance. The dimensions of the antenna are 59.6 x 45.6 x 1.56 mm^3 which is quite large compared to the proposed antenna. The antenna demonstrates an impedance bandwidth of 95 MHz at a -10 dB level. Additionally, in simulation, it exhibits a notable peak gain value of 6.8 dBi. In [15], a compact antenna for multiband applications introduced with cut slots and parasitic patch fabricated on FR-4 substrate has been presented. The total dimensions 44.4 x 55.60 x 1.6 mm^3 are used and simulated on CST software. The antenna presented has the capability of operating in ITU band, IEEE 802.11a system, WLAN,

satellite communications, Aeronautical radio navigation, maritime applications. A compact microstrip antenna with V-shaped cut connected to U-slot has been proposed fabricated on FR-4 substrate and simulated on CST software [16]. The dimension is 40 x 40 x 1.6 mm^3 much larger than proposed antenna and is designed for super high frequencies such as to operate for Satellite Communications, Citizens Broadband, C-band and X-band applications etc. The antenna generates resonance in multiple bands at frequencies of 3.7164 GHz, 5.6461 GHz, 7.8485 GHz, and 9.3645 GHz. The return loss values for these bands are -26 dB, -17.418 dB, -39.031 dB, and -24.44 dB, accompanied by corresponding gain values of 3.8 dBi, 2.078 dBi, 4.662 dBi, and 3.391 dBi, respectively. An inset-fed rectangular patch antenna to enhance the bandwidth using degraded structure in the ground plane is presented in [17]. The DGS is responsible for bandwidth enhancement with the overall patch dimension of 42 x 50 mm^2. A return loss bandwidth of 36.7% at a -10 dB level and a consistent gain of 3.4 dB have been successfully attained. A triple band inset-fed microstrip antenna is having c-shaped slot on the patch has been presented in [18] incorporated with partial ground structure. The antenna possesses the dimension of 49 x 38 x 1.6 mm^3 and can be used for DCS, WLAN, Bluetooth, LTE and other communication bands. The bandwidth of 25%, 13% and 5.7% are achieved. [19] introduces an improved bandwidth multi-band slot antenna tailored for applications in 4G-LTE/WiMAX/WLAN, as well as S/C/X-bands. The inclusion of embedded E-shaped and T-shaped stubs in the antenna's design facilitates the attainment of multiple resonating bands while significantly enhancing the impedance bandwidth. The bandwidths achieved are 29%, 6.67%, 20.2% and 25.6% with the gain of 3.9, 3.6, 5.01 and 5.4 dBi. A planar multi-band slot antenna has been devised in [20] to accommodate GPS, WLAN, S-band, C-band, and X-band frequencies. The antenna configuration comprises a radiating slot incorporating a T-shaped feed patch, along with two inverted T-shaped stubs and two E-shaped stubs. A dual-wideband fractal antenna has been developed to serve Bluetooth, WiMAX, WLAN, C, and X band applications [21]. This antenna design incorporates a circular resonator with square slots and utilizes a ground plane featuring a gap line. The integration of the gap line is aimed at enhancing both gain and bandwidth within a compact structure, measuring just 40 × 34 × 1.6 mm³. The proposed design in [22] includes a J slot on a rectangular patch, energized by an inset feeding. The results of the designed antenna demonstrate its capability to achieve multiband functionality, catering not only to WIFI, LTE-U, and WIMAX applications but also extending to C band, X band, and Ku band applications. A compact dual-band CPW-fed antenna which incorporates two asymmetrical coplanar ground planes, enhancing its capability to operate across diverse frequency bands has been presented [23]. The inclusion of an inverted L-shaped parasitic slit contributes to the antenna's ability to generate two well-defined operating bands. This versatile design accommodates various service bands, such as S-, C-, WiMAX, WLAN, UWB, and X-band communication systems. Despite its small footprint measuring 24.5 × 20 mm^2 and a uniplanar profile, the antenna efficiently covers a broad spectrum of frequencies. Furthermore, certain antennas exhibit considerable volumetric dimensions and intricate footprints. Consequently, there is a need to introduce an antenna capable of functioning across a range of frequencies, including S-band, WiMAX, WLAN, C-band and X-bands.

In this paper, a compact inset-fed pentaband microstrip antenna has been proposed which can operate for UMTS, WLAN, WiMAX, C- and X-band applications. The slotted structure and the inset feeding are responsible for generating the five operating bands. The gains achieved at these five bands are very much better. The antenna is mounted on the FR4 substrate and a 50 Ω microstrip feeding line has been used. The design, evolution, parametric analysis, measured results are discussed and well presented in the upcoming sections.

2. Antenna Design

The geometry of the proposed novel design of a compact inset-fed pentaband microstrip antenna with all the depicted nomenclatures of the design parameters has been shown in Fig. 1. The proposed antenna is fabricated on the FR4 substrate with the height of 1.6 mm, dielectric constant of 4.4 and loss tangent of 0.02 since a wider bandwidth and increased directivity are achievable with a lower dielectric constant and reduced loss tangent. The cost-effectiveness and ready availability of these characteristics in the market, coupled with significant return loss, make it an attractive choice. FR-4, known for its robust mechanical strength and dimensional stability, is opted for the proposed antenna to ensure the structural integrity is maintained. As shown in Figure 1, the antenna is comprised of four slots of equal dimensions, i.e., of same length and width and are apart from each other equally. The length and width of slots are denoted by Sl_L and Sl_W respectively and the distance between these slots is denoted by t2. The penetration of feed into the patch known as inset feeding has the length and width shown in figure as IN_L and IN_W. Lp and Wp denote the length and width of rectangular patch while Lsub, Wsub and Lg denote the length of substrate, width of substrate and length of ground. This is a full ground structure with same dimensions as of substrate. LF1 and WF1 are the length and width of feedline and LF2 and WF2 are of quarter-wave transformer transmission line. To match real load impedance with different source impedance, the quarter-wave transformer is very useful and simple method which is frequently used in antenna design [24]. Table 1 displays the dimensions of the prototype antenna. All the dimensions are in mm. The methodology proposed for designing the antenna and for the optimum dimensions chosen in this article has been presented as a flow chart in Fig.2.
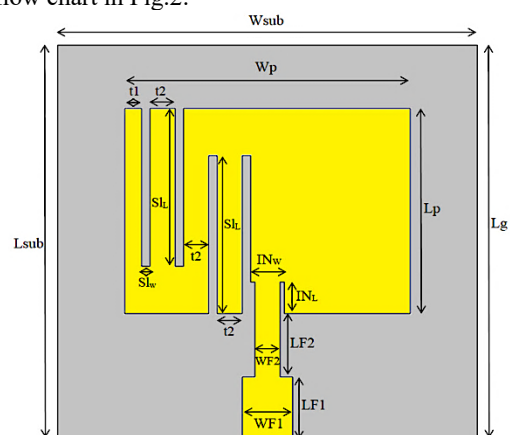

Fig. 1. Geometrical design of the proposed antenna.

The useful antenna equations that can be used to design and fabricate an antenna are [1]:
The width of the patch Wp can be calculated as:

$$W_p = \frac{c}{2f_o\sqrt{\frac{\varepsilon_r+1}{2}}} \tag{1}$$

The effective dielectric constant, ε_{reff} can be calculated as:

$$\varepsilon_{reff} = \frac{\varepsilon_r+1}{2} + \frac{\varepsilon_r-1}{2}\left[1 + 12\frac{h}{W_p}\right]^{1/2} \tag{2}$$

The length of the patch can be calculated as:

$$L_p = L_{eff} - 2\Delta L \tag{3}$$

where, L_{eff} is the effective length of patch given as

$$L_{eff} = \frac{c}{2f_o\sqrt{\varepsilon_{reff}}} \tag{4}$$

and ΔL is the extension in length due to fringing given as

$$\Delta L = 0.412h\frac{(\varepsilon_{reff}+0.3)(\frac{W_p}{h}+0.264)}{(\varepsilon_{reff}+0.258)(\frac{W_p}{h}+0.8)} \tag{5}$$

The length and width of the substrate Lsub and Wsub are equal to that of the ground plane Lg and Wg given as

$$L_g = 6h + L_p \tag{6}$$

$$W_g = 6h + W_p \tag{7}$$
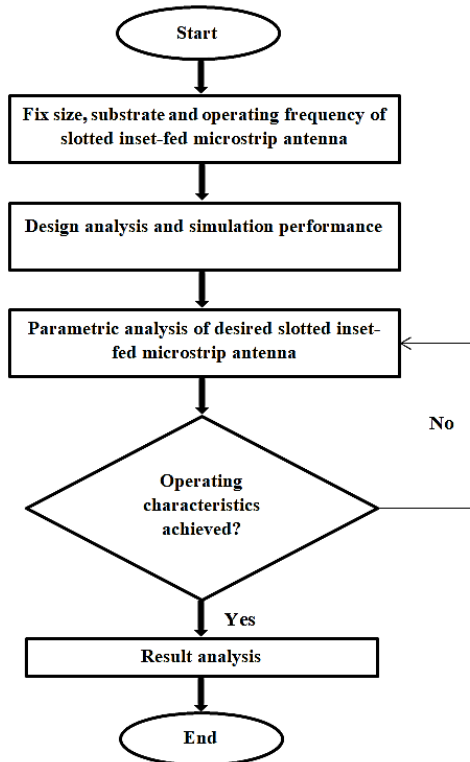
Fig. 2. Flow-chart of proposed methodology.

Table 1. Geometrical Dimensions of the Proposed Antenna (all values are in mm).

Parameter	Value	Parameter	Value
Lsub	25	Sl$_W$	0.5
Wsub	25	IN$_L$	2
Lg	25	IN$_W$	2
Lp	13	LF1	4
Wp	17	WF1	3
t1	1	LF2	4
t2	2	WF2	1.5
Sl$_L$	10		

Fig. 3 shows the reflection coefficient of the proposed antenna. The antenna resonates at five frequencies giving out good impedance bandwidth and better gain & VSWR. The frequencies at which the antenna resonates are 2.1 GHz, 5.2 GHz, 6.3 GHz, 7.8 GHz and 10.4 GHz suitable for UMTS, WLAN, WiMAX, C-band and X-band applications.
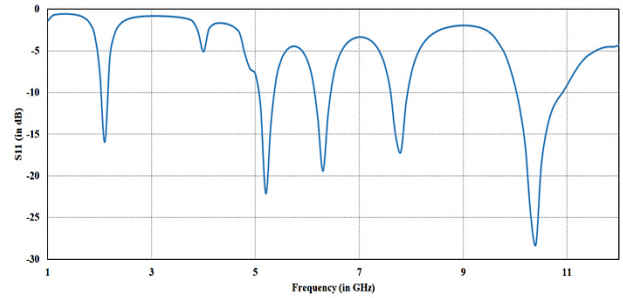

Fig. 3. Return Loss of the Proposed Antenna

3. Evolution of Antenna

In this section, the geometrical progress of the antenna is shown to achieve the proposed antenna design in Fig. 4 with the respective return losses in Fig. 5. In the beginning, the simple rectangular patch is designed with inset and modified feeding structure and full ground depicted as Antenna 1 in Fig. 4. It is evident from the simulated reflection coefficient graph in the Fig. 5 that this antenna exhibits only two resonant frequencies and that too at around 5.1 GHz with -17 dB and at 10 GHz with -34 dB. This shows a good dual frequency and simple structure but the drawback is that it doesn't fully cover the 5.2 GHz bands.

Then, a single slot is cut towards the left of the rectangular patch from the upper side. This structure is shown in the graph as Antenna 2 in Fig. 4. This structure incorporates two bands in the graph of simulated reflection coefficient and can also be seen in the Fig. 5. The resonant frequencies are at 5.1 GHz and 9.9 GHz.

Now, when one more slot of the same length and width beside the first one is cut spaced by t2 shown in Fig. 4 as Antenna 3, then it can be seen from the figure that four bands are achieved as depicted in Fig. 5. The resonant frequencies of these three bands are at 5.1 GHz, 8.3 GHz, 9.9 GHz and 11.4 GHz. After that, in the next step, again a slot of same length and width at a distance of t2 from the second slot is cut but this time from the bottom of the patch as shown in Fig. 4 as Antenna 4. This design resonates at four frequencies, i.e., at 2.2 GHz, 5.2 GHz, 5.7 GHz and 10.2 GHz. Finally, when one more slot of same length and width is made on the patch spaced by t2 from third slot depicted as Proposed Antenna in Fig. 4, five bands are generated with good impedance bandwidth and better gain. These bands are (2.0-2.2)/2.1 GHz, (5.0-5.4)/5.2 GHz, (6.1-6.5)/6.3 GHz, (7.5-8.0)/7.8 GHz and (9.9-11.1)/10.4 GHz with the return loss of -16 dB, -22.1 dB, -19.4 dB, -17.1 dB and -28.2 dB respectively.
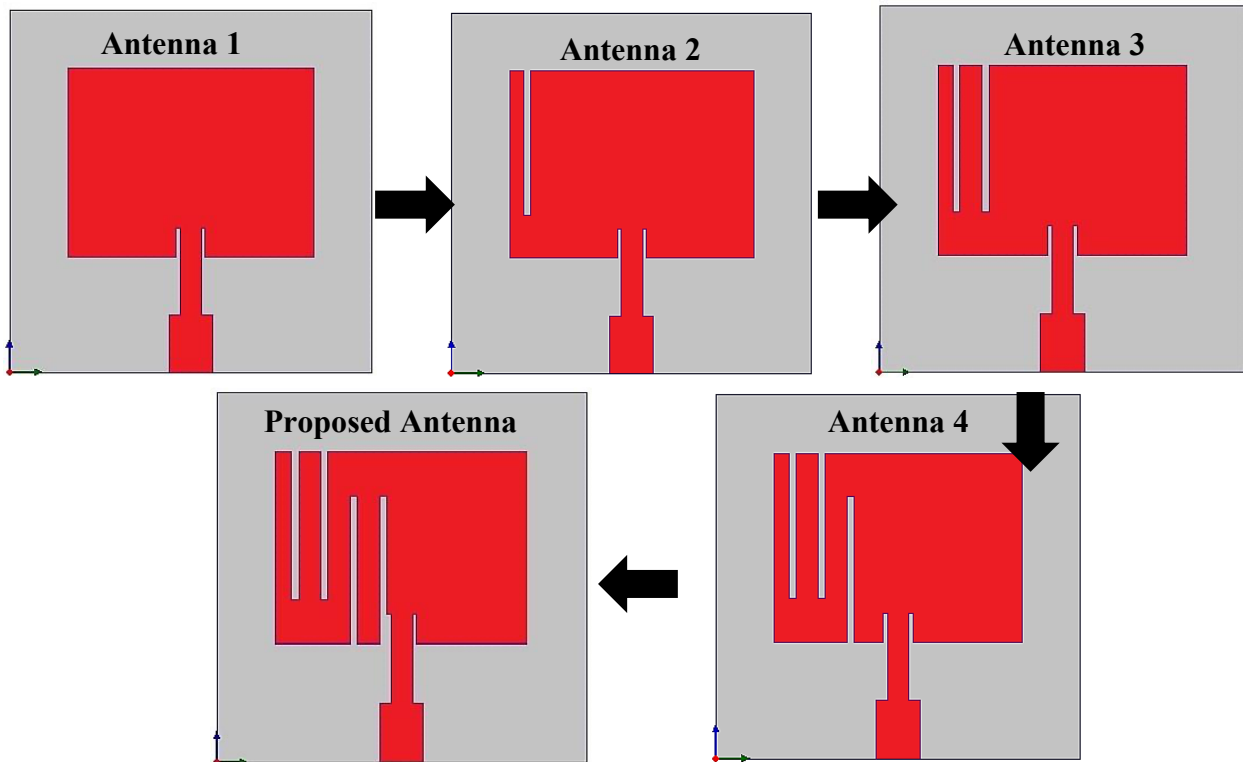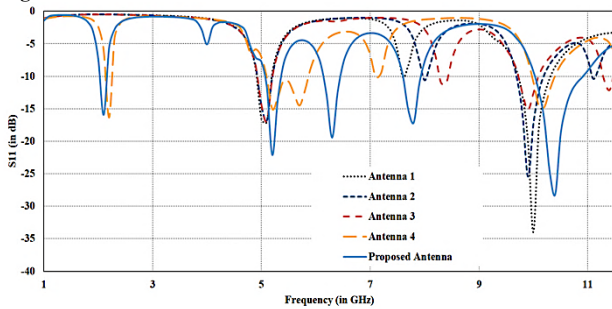
Fig. 4. Evolution of Antenna

Fig. 5. Return losses of antenna evolution.

4. Result and Discussion

The proposed antenna presented in this article has total dimensions of 25 x 25 x 1.6 mm³. The antenna is having very compact size and also of very low profile. The good bandwidth, the better gain and also the VSWR which comes out to be very good are obtained of the proposed antenna. The frequency bands the antenna covers are (2.0-2.2)/2.1 GHz, (5.0-5.4)/5.2 GHz, (6.1-6.5)/6.3 GHz, (7.5-8.0)/7.8 GHz and (9.9-11.1)/10.4 GHz suitable for UMTS, WLAN, WiMAX, C-band and X-band applications. The impedance bandwidths of the simulation are 9.5%, 7.6%, 6.3%, 6.4% and 11.5% respectively.
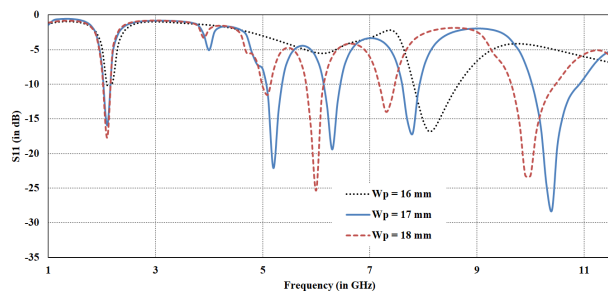
Fig. 6. S11 vs Frequency plot for Variation in the Width of the Patch.

4.1 Parametric Analysis

Fig. 6 demonstrates the plot of reflection coefficient for the variation in the width of the patch. The variation is taken from 16 mm to 18 mm and the respective reflection coefficient has been shown in the figure for comparison to state that the value taken is the optimum one. When the value of Wp is 16 mm, then antenna resonates only once at 8.1 GHz with -16.8 dB return loss. Now, the value of 18 mm is taken for which antenna resonates at four frequencies at 2.1 GHz with -15.9 dB, 6 GHz with -25.32 dB, 7.3 GHz with -13.9 dB and at 10 GHz with -23.18 dB return loss. But as the value 17 mm is taken for patch width, the antenna gives out fives resonant frequencies at 2.1, 5.2, 6.3, 7.8 and 10.4 GHz. Hence, Wp with 17 mm gives the optimum results.
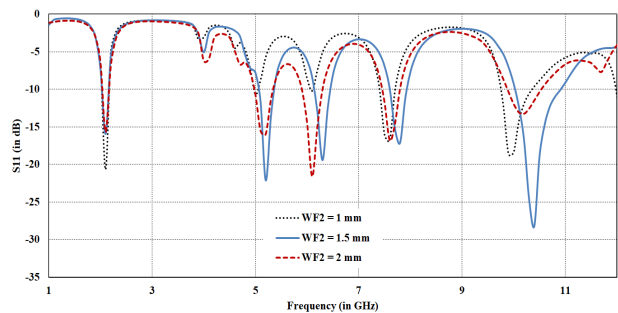

Fig. 7. S11 vs Frequency plot for Variation in the Width of quarter wave transformer.

Fig. 7 shows the reflection coefficients of the proposed antenna for different values width of the quarter wave transformer. Here the variation in width is taken from 1 mm to 2 mm with the step size of 0.5 mm. Now, the value 1 mm taken for WF2, antenna gives out only three bands and that too resonates at 2.1 GHz with -20.6 dB, 7.6 GHz with -16.8 dB and at 9.9 GHz with -18.6 dB return losses. When the value for WF2 is taken 2 mm, then the antenna gives out five bands but with very low return losses, i.e., at 2.1 GHz with -15.6 dB, 5.2 GHz with -15.9 dB, 6.1 GHz with -21.6 dB, 7.6 GHz with -16.7 dB and at 10.2 GHz with -13.2 dB. But, when the value of width of second feed is taken as 1.5 mm, then five

bands with good return losses are obtained and hence, this value of WF2 gives optimum results.

The reflection coefficient graph for the variation taken in the substrate height is presented in the Fig. 8. The variation is done from 0.8 mm to 1.6 mm with step of 0.8 mm. The value of 0.8 mm for the height of substrate gives out only three resonant frequencies which are at 1.8 GHz with -20.2 dB, 7.9 GHz with -18.3 dB and at 10.3 GHz with -16.2 dB return losses. Now, when the height of substrate is given the value of 1.6 mm, then the desired and the optimum results of five bands with better gain, VSWR and good bandwidth are obtained.
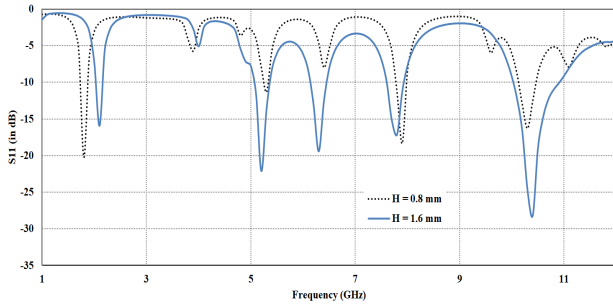
Fig. 8. S11 vs Frequency plot for variation in the Substrate Height.

Fig. 9 illustrates the reflection coefficient graph for the parametric analysis done for variation in the ground plane length Lg. For all the three values that has been taken, the antenna resonates at five frequencies but at Lg with the value of 25 mm, gives the better return loss values when compared to other two dimensions as this is clearly visible from the Fig. 9. Hence, the value 25 mm for Lg is the optimum one.
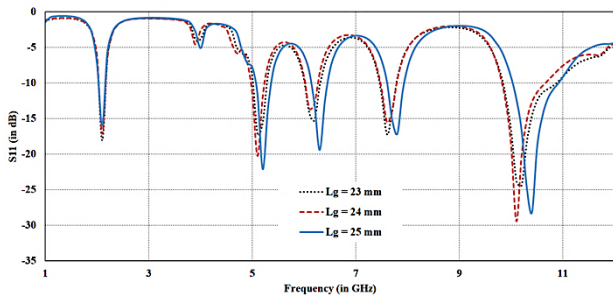

Fig. 9. S11 vs Frequency plot for variation in the length of ground plane.
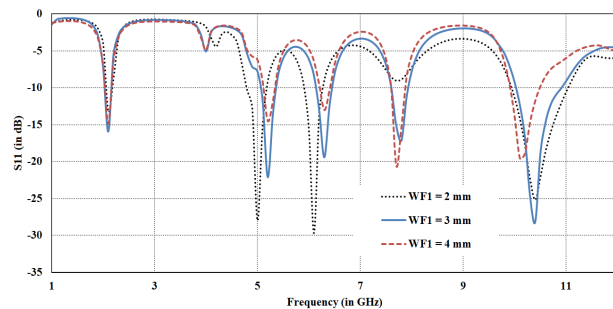

Fig. 10. S11 vs frequency plot for the variation in the width of transmission line.

The plot for the WF1 which is the width of the transmission line is presented in Fig. 10 with the values varied from 2 mm to 4 mm. there are four resonances for the 2 mm width which are at 2.1 GHz, 5 GHz, 6.1 GHz and 10.4 GHz. When the value of WF1 is taken 4 mm then, there are five bands generated but they are having less return losses when compared to that of those which are generated when the value

is taken as WF1=3 mm. Hence, the 3 mm transmission line width is the optimum one.
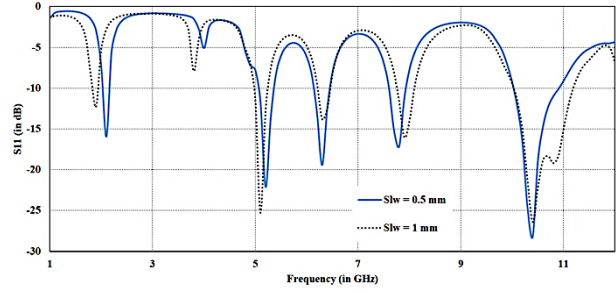

Fig. 11. S11 vs frequency plot for the variation slot width.

Fig. 11 demonstrates the graph of the reflection coefficient when the width of the slot made onto the patch has been varied from 0.5 to 1 mm. Since, the value of 1 mm for Slw is also giving out the five bands but they are having less return losses as can be seen from the plot. Hence, value of Slw = 0.5 mm provides the five bands with good return loss and bandwidth along with the better gain.

4.2 Surface Current Distribution
Fig. 12 demonstrates the surface current distribution at 2.1 GHz and 5.2 GHz for the antenna proposed in this article. The surface current distribution at rest of the resonant frequencies, i.e., at 6.3 GHz, 7.8 GHz and 10.4 GHz is shown in the Fig. 13. It is evident from the Figure 12 that at 2.1 GHz the maximum current is flowing through the slotted structure between the second and the third slots. From the same figure, the maximum current at 5.2 GHz is flowing through the all the slots and whole of the patch and also through the feeding structure.
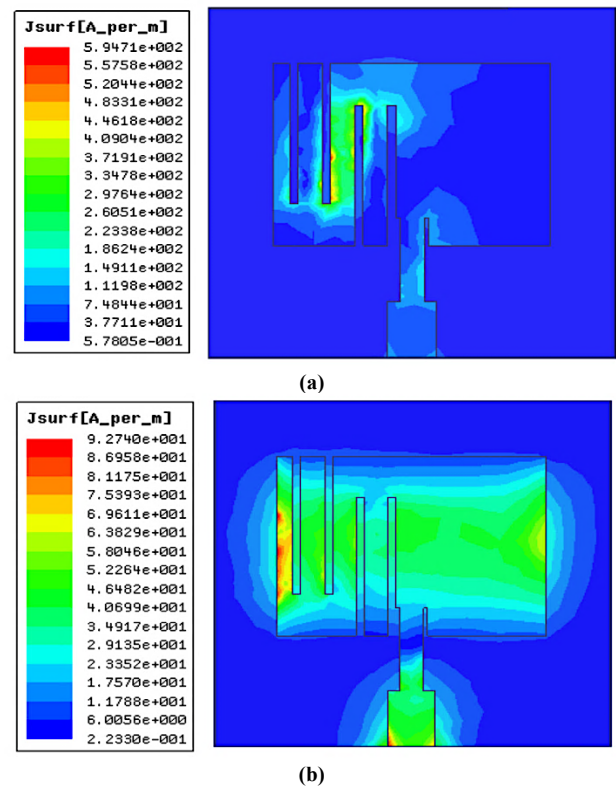

(a)

(b)

Fig. 12. Surface Current Distribution of Proposed Antenna at (a) 2.1 GHz and (b) 5.2 GHz.

Now, from the Fig. 13, it can be clearly seen that the maximum current at 6.3 GHz is flowing through the third and fourth slots, the feeding structure and also through the right side of the patch. The current distribution at 7.8 GHz is clearly

seen flowing from the feeding structure and inset area. At 10.4 GHz, the maximum current distribution is taking place through the second feeding structure and also through the upper right of the rectangular patch. The red indication shows the higher current distribution.
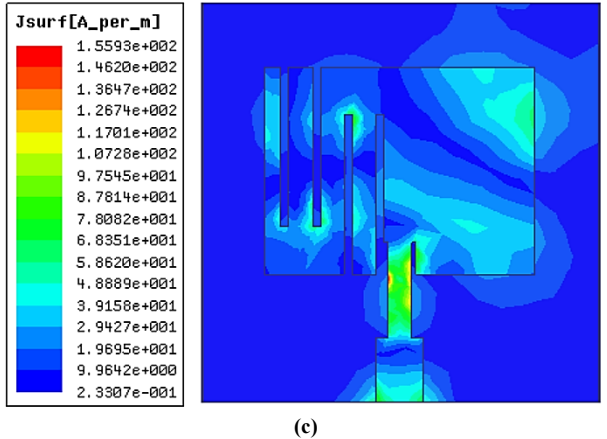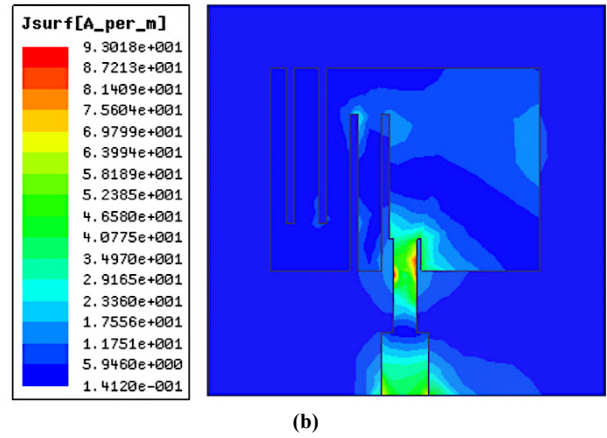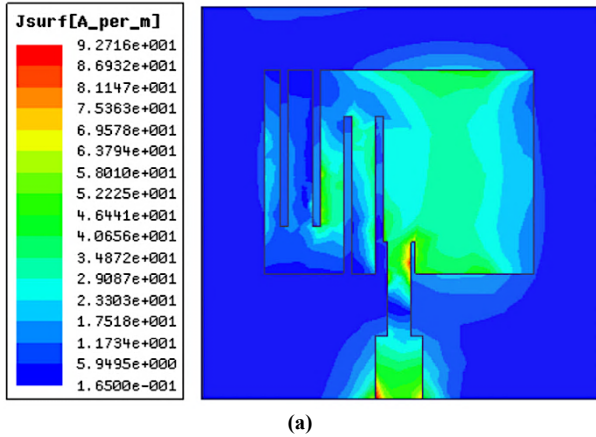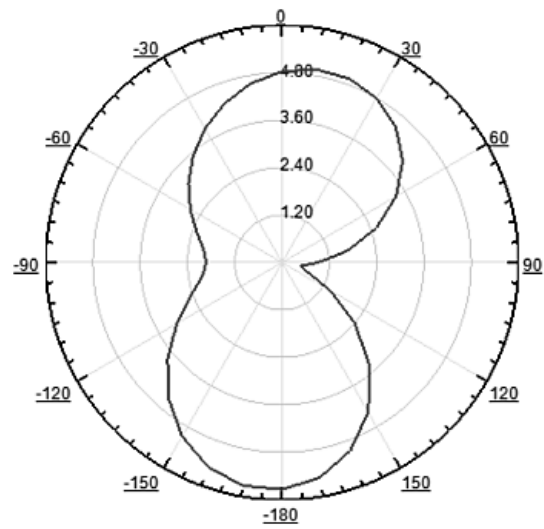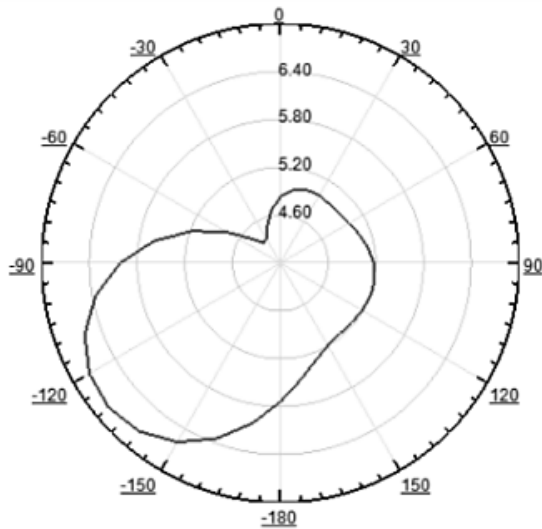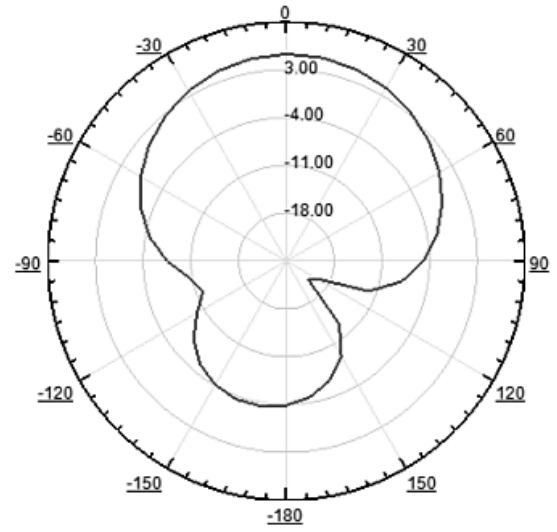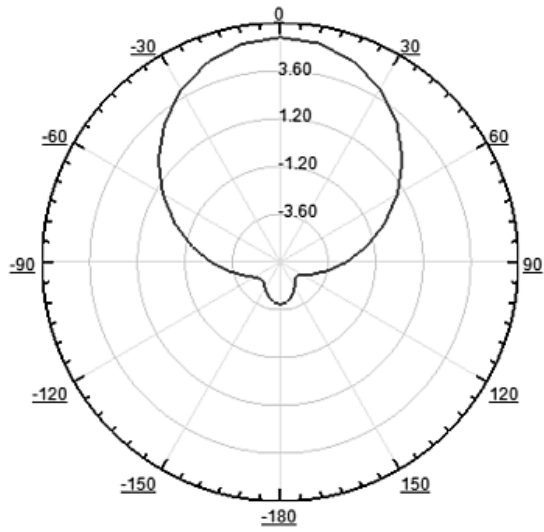

(a)

(b)

(c)

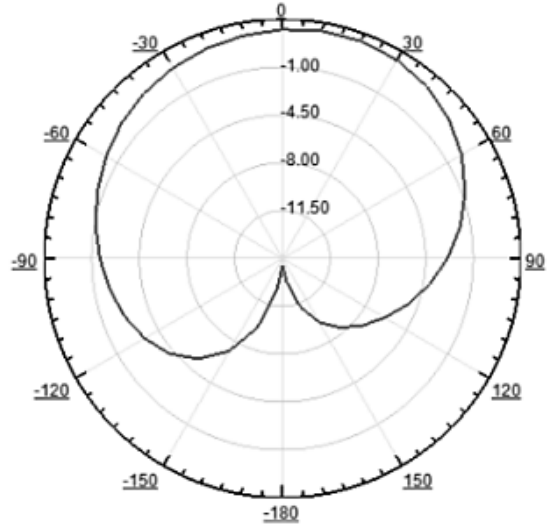**Fig. 13.** Surface Current Distribution of Proposed Antenna at (a) 6.3 GHz, (b) 7.8 GHz and (c) 10.4 GHz.

4.3 Radiation Pattern
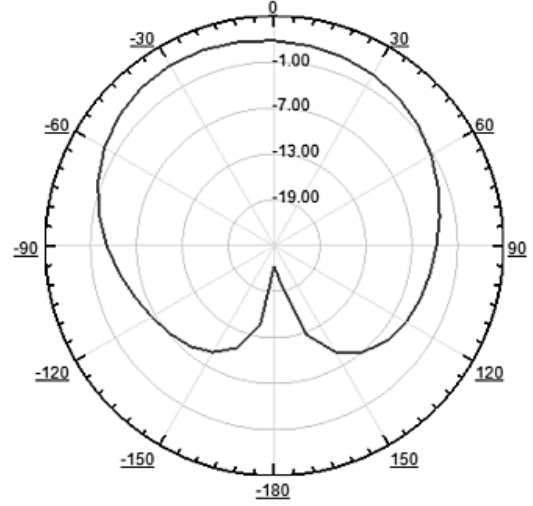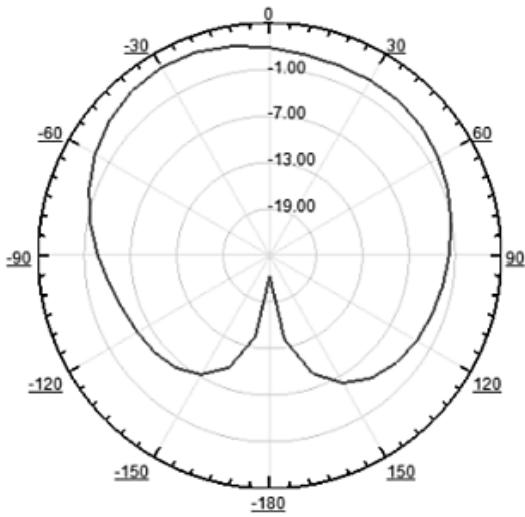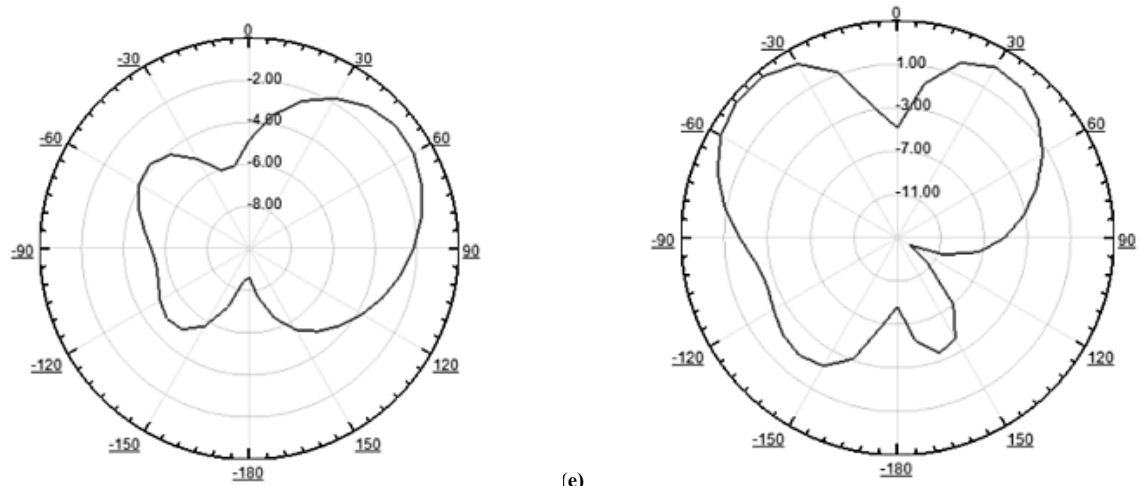

(a)

(b)

(c)

(d)

(e)
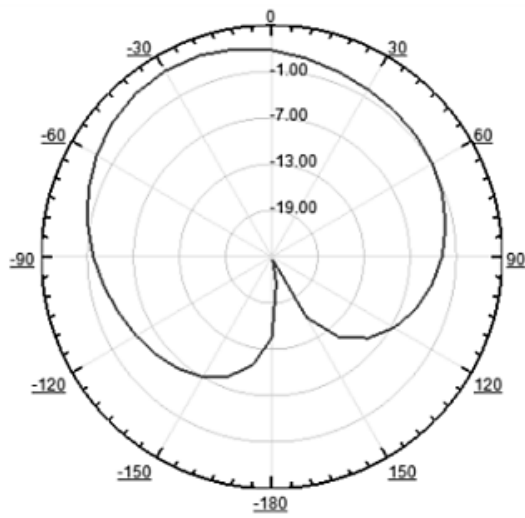
Fig. 14. Radiation Pattern at (a) 2.1 GHz, (b) 5.2 GHz, (c) 6.3 GHz, (d) 7.8 GHz and (e) 10.4 GHz.

Fig. 14 displays the radiation patterns at 2.1, 5.2, 6.3, 7.8 and 10.4 GHz, respectively. One can see from the figure that good omnidirectional radiation property is shown. The radiation pattern is taken at phi= 0 degree and phi= 90 degrees for all the resonant frequencies. In the left side of the figure, the E-plane pattern is shown and in the right hand of the figure, H-plane pattern is shown. It is very much evident from the Fig. 9 that antenna radiates bi-directional for 2.1 GHz, uni-directional for 5.2 GHz and dipole like radiation for 6.3, 7.8 and 10.4 GHz in E-plane and for H-plane antenna radiation pattern is bi-directional for 2.1 and 5.2 GHz, and dipole like pattern for 6.3, 7.8 and 10.4 GHz.

4.4 Gain
The simulated gain plot obtained at the resonant frequencies has been presented in the Fig. 15. The gain obtained at 2.1 GHz, 5.2 GHz, 6.3 GHz, 7.8 GHz and 10.4 GHz are 7.13 dBi, 5.2 dBi, 2.71 dBi, 3.12 dBi and 5.17 dBi, respectively.
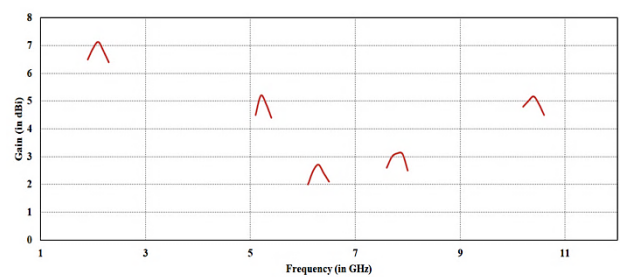

Fig. 15. Gain Plot of the proposed Antenna.

Table 2 exhibits the comparison between the proposed antenna and the already existing antennas in the literature in respect to size, frequency bands and bandwidth.

Table 2. Comparison between the existing antennas in the literature and proposed antenna.

References	Antenna Size (mm³)	Frequency Bands	Bandwidth (%)	Gain (dBi)
[18]	49x38x1.6	Triple-band	25, 13 and 5.7.	NR
[25]	22x40x1.6	Quad-band	36, 31, 15 and 22.	2.05, 2.83, 2.08 and 2.96.
[26]	45x17x1.6	Dual-band	2.89 and 2.78.	1.18 and 2.1.
[27]	57.2x31.2x1.6	Quad-band	7.78, 8.16, 18.86 and 16.91.	-8.12, -1.31, 1.46 and 3.66.
[19]	56x44x1.6	Quad-band	29, 6.67, 20.2 and 25.6.	3.9, 3.6, 5.01 and 5.4.
[28]	32x37.2x1.6	Triple-band	12.5, 7.42 and 6.36.	2.25, 3.72 and 2.71.
[29]	65x85x0.78	Dual-band	17.3 and 26.5.	5.4 and 5.2.
Proposed Antenna	**25x25x1.6**	**Penta-band**	**9.5, 7.6, 6.3, 6.4 and 11.5.**	**7.13, 5.2, 2.71, 3.12 and 5.17.**

5. Measured Result

5.1 Reflection Coefficient and Bandwidth:
The performance analysis of proposed multiband antenna is done in terms of S11 and VSWR. The physical picture of proposed antenna fabricated has been shown in the Fig. 16. The simulated and the measured reflection coefficient S11 of the proposed antenna has been presented in the Fig. 17. The testing of the proposed antenna has been conducted using an anechoic material place around the Anritsu VNA, including return loss and VSWR. The return loss and VSWR has been

measured and tested by Anritsu VNA Master MS2037C/2 in which the proposed fabricated antenna has been connected to VNA for getting the measurements of reflection coefficients and VSWR and the results are compared with the simulated results. Some of the discrepancies can be seen and that could be due to the fabrication tolerances, material properties, connector impedance and measurement tolerances factors.

It is evident from the figure that the antenna can operate in five distinct frequency bands resonating at (1.88 – 2.03)/1.96 GHz with -18 dB, (5.09 – 5.32)/5.17 GHz with -13 dB, (6.13 – 6.51)/6.36 GHz with -14 dB, (7.48 – 7.99)/7.77

GHz with -19 dB and (9.86 – 11.42)/ 10.16 GHz with -26 dB return loss. The respective impedance bandwidths of the measured result are 7.7%, 4.4%, 6%, 6.6% and 15.4%.
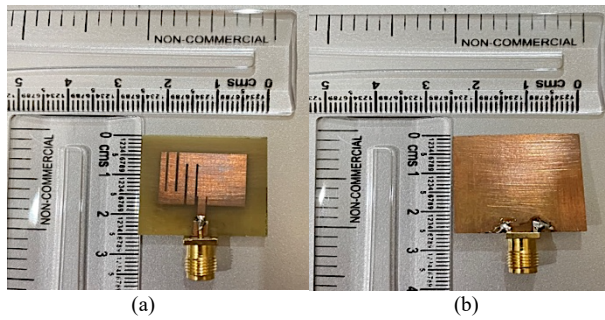

(a)   (b)

Fig. 16. Fabricated Model of the Proposed Antenna.

5.2 VSWR

Fig. 18 demonstrates the VSWR plot of the antenna both for simulated and the measured one. It is evident from the plot that at all the resonant frequencies, the antenna is matched. For the simulated plot the VSWR value at 2.1 GHz, 5.2 GHz, 6.3 GHz, 7.8 GHz and 10.4 GHz are 1.79, 1.36, 1.86, 1.43 and 0.67, respectively. And VSWR values for the measured plot at 1.96 GHz, 5.17 GHz, 6.36 GHz, 7.77 GHz and 10.16 GHz are 2.00, 1.55, 1.50, 1.26 and 1.10.
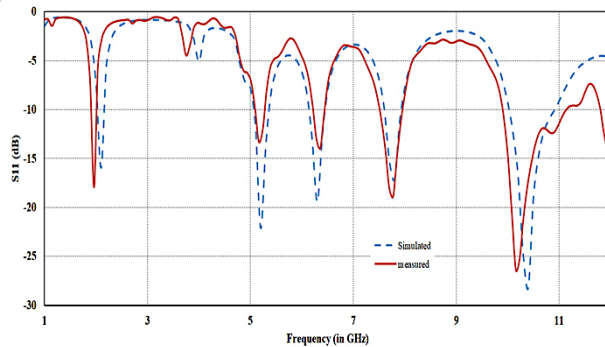

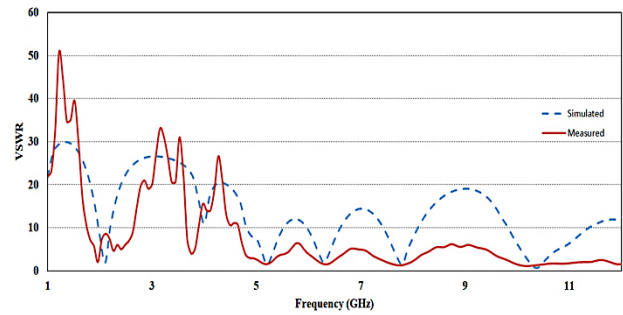**Fig. 17.** Simulated and Measured Reflection Coefficient of the proposed Antenna.

Fig. 18. VSWR (Simulated and Measured Plot of the Proposed Antenna.

6. Conclusion

The research article has documented the successful development of a compact slotted pentaband inset-fed microstrip antenna designed to operate for UMTS, WLAN, WiMAX, C-band and X-band applications with the dimensions of 25 x 25 x 1.6 mm^3. The paper provides a comprehensive account of the antenna's evolution, highlighting the steps taken to achieve its current design. This novel antenna maintains excellent performance across five frequency bands while achieving a significant reduction in size. It offers a good impedance bandwidths which are 9.5%, 7.6%, 6.3%, 6.4% and 11.5% respectively and relatively high gains of 7.13 dBi, 5.2 dBi, 2.71 dBi, 3.12 dBi and 5.17 dBi at 2.1 GHz, 5.2 GHz, 6.3 GHz, 7.8 GHz and 10.4 GHz respectively. Furthermore, the proposed antenna demonstrates stable radiation patterns in the five frequency bands, making it suitable for various wireless communication applications.

References

[1] .C. A. Balanis, *Balanis' advanced engineering electromagnetics*, Third edition. Hoboken, New Jersey: John Wiley & Sons, 2024.

[2] Jing Pei, An-Guo Wang, Shun Gao, and Wen Leng, "Miniaturized Triple-Band Antenna With a Defected Ground Plane for WLAN/WiMAX Applications," *Antennas Wirel. Propag. Lett.*, vol. 10, pp. 298–301, Apr. 2011, doi: 10.1109/LAWP.2011.2140090.

[3] R. H. Patel, A. Desai, and T. K. Upadhyaya, "An electrically small antenna using defected ground structure for RFID, GPS and IEEE 802. 11 A/B/G/S applications," *PIER Letters*, vol. 75, pp. 75–81, Jan. 2018, doi: 10.2528/PIERL18021901.

[4] D. Sarkar, K. Saurav, and K. V. Srivastava, "Multi-band microstrip-fed slot antenna loaded with split-ring resonator," *Electron. lett.*, vol. 50, no. 21, pp. 1498–1500, Oct. 2014, doi: 10.1049/el.2014.2625.

[5] A. Desai and T. Upadhyaya, "Transparent dual band antenna with μ-negative material loading for smart devices," *Micro & Optical Tech Letters*, vol. 60, no. 11, pp. 2805–2811, Nov. 2018, doi: 10.1002/mop.31474.

[6] T. K. Upadhyaya, S. P. Kosta, R. Jyoti, and M. Palandoken, "Negative refractive index material-inspired 90-deg electrically tilted ultra wideband resonator," *Opt. Eng*, vol. 53, no. 10, p. 107104, Oct. 2014, doi: 10.1117/1.OE.53.10.107104.

[7] T. K. Upadhyaya, S. P. Kosta, R. Jyoti, and M. Palandöken, "Novel stacked μ -negative material-loaded antenna for satellite applications," *Int. J. Microw. Wireless Technol.*, vol. 8, no. 2, pp. 229–235, Mar. 2016, doi: 10.1017/S175907871400138X.

[8] N. Bayatmaku, P. Lotfi, M. Azarmanesh, and S. Soltani, "Design of Simple Multiband Patch Antenna for Mobile Communication Applications Using New E-Shape Fractal," *Antennas Wirel. Propag. Lett.*, vol. 10, pp. 873–875, May 2011, doi: 10.1109/LAWP.2011.2165195.

[9] M. A. Al-Joumayly, S. M. Aguilar, N. Behdad, and S. C. Hagness, "Dual-Band Miniaturized Patch Antennas for Microwave Breast Imaging," *Antennas Wirel. Propag. Lett.*, vol. 9, pp. 268–271, Apr. 2010, doi: 10.1109/LAWP.2010.2045871.

[10] Mohammad Matin and A. Sayeed, "A design rule for inset-fed rectangular microstrip patch antenna," *WSEAS Trans. Commun.*, Vol. 9, No. 1, pp 63-72, Jan. 2010.

[11] Devan Bhalla and Krishan Bansal, "Design of a Rectangular Microstrip Patch Antenna Using Inset Feed Technique," *IOSR J. Electron. & Commun. Eng. (IOSR-JECE)*, Vol. 7, No. 4, pp. 08-13, Oct. 2013.

[12] S. M. Asif, A. Iftikhar, S. M. Khan, M. Usman, and B. D. Braaten, "An E-shaped microstrip patch antenna for reconfigurable dual-band operation," *Microw. Opt. Technol. Lett.*, vol. 58, no. 6, pp. 1485–1490, Jun. 2016, doi: 10.1002/mop.29814.

[13] L. C. Paul, M. M. Ur Rashid, M. M. Mowla, M. Morshed, and K. Sarkar, "Performance enhancement of an inset feed rectangular microstrip patch antenna by adjusting feeding position for wireless applications," in *3rd Int. Conf. Electric., Electr., Eng. Trends, Comm., Optimiz. Sc. (EEECOS 2016)*, Tadepalligudem, India: Institution of Engineering and Technology, 2016. doi: 10.1049/cp.2016.1549.

[14] W. Farooq, M. Ur-Rehman, Q. H. Abbasi, K. Q. Maqbool, and K. Qaraqe, "Study of a microstrip patch antenna with multiple circular slots for portable devices," in *2015 IEEE 8th GCC Conf. Exhib.*, Muscat, Oman: IEEE, Feb. 2015, pp. 1–4. doi: 10.1109/IEEEGCC.2015.7060037.

[15] A. Dadhich, J. K. Deegwal, S. Yadav, and M. M. Sharma, "Design of multi-band antenna with cut slots and parasitic patch for wireless communication," in *2017 IEEE Appl. Electromagn. Conf. (AEMC)*, Aurangabad: IEEE, Dec. 2017, pp. 1–2. doi: 10.1109/AEMC.2017.8325631.

[16] A. Dadhich, J. K. Deegwal, and M. M. Sharma, "Study and design of multiband antenna with V and U slot on patch for wireless application," in *2017 IEEE Appl. Electromagn. Conf. (AEMC)*, Aurangabad: IEEE, Dec. 2017, pp. 1–2. doi: 10.1109/AEMC.2017.8325629.

[17] C. Mbinack, B. Bodo, J. A. Eyébé Fouda, and E. Tonye, "Inset-fed rectangular MICROSTRIP patch antenna bandwidth enhancement," *Micro & Optical Tech Letters*, vol. 61, no. 2, pp. 562–567, Feb. 2019, doi: 10.1002/mop.31565.

[18] B. Kumawat, S. Yadav, M. M. Sharma, J. K. Deegwal, and A. Dadhich, "Tri-Band Rectangular Patch Antenna with C Slot," in *2019 IEEE Indian Conf. Antenn. Propog. (InCAP)*, Ahmedabad, India: IEEE, Dec. 2019, pp. 1–3. doi: 10.1109/InCAP47789.2019.9134584.

[19] B. K. Sah, G. Singla, and S. Sharma, "Design and development of enhanced bandwidth multi-frequency slotted antenna for 4G-LTE/WiMAX/WLAN and S/C/X-band applications," *Int J RF Microw Comput Aided Eng*, vol. 30, no. 7, Jul. 2020, doi: 10.1002/mmce.22214.

[20] S. S. Indharapu, M. B. Abhishikth, and S. Chilukuri, "A Multiband Slot Antenna for Wireless Communication Applications," in *2018 9th Int. Conf. Comp., Commun. Netw. Techn. (ICCCNT)*, Bangalore: IEEE, Jul. 2018, pp. 1–5. doi: 10.1109/ICCCNT.2018.8493996.

[21] M. Marzouk *et al.*, "Ultra-Wideband Compact Fractal Antenna for WiMAX, WLAN, C and X Band Applications," *Sensors*, vol. 23, no. 9, p. 4254, Apr. 2023, doi: 10.3390/s23094254.

[22] N. Nitin, J. A. Ansari, and N. Agrawal, "Inset Fed J Slotted Microstrip Multiband Antenna for WiFi /LTE /WiMAX/ C Band/X Band/Ku Band Applications," in *2020 IEEE Stud. Conf. Eng. Sys. (SCES)*, Prayagraj, India: IEEE, Jul. 2020, pp. 1–6. doi: 10.1109/SCES50439.2020.9236752.

[23] Md. M. Alam, R. Azim, N. M. Sobahi, A. I. Khan, and M. T. Islam, "A dual-band CPW-fed miniature planar antenna for S-, C-, WiMAX, WLAN, UWB, and X-band applications," *Sci Rep*, vol. 12, no. 1, Art. No. 7584, May 2022, doi: 10.1038/s41598-022-11679-7.

[24] I. J. Bahl and P. Bhartia, *Microstrip antennas*. in The Artech House microwave library. Dedham, Mass: Artech House, 1980.

[25] S. A. A. Shah, M. F. Khan, S. Ullah, A. Basir, U. Ali, and U. Naeem, "Design and Measurement of Planar Monopole Antennas for Multi-Band Wireless Applications," *IETE J. Res.*, vol. 63, no. 2, pp. 194–204, Mar. 2017, doi: 10.1080/03772063.2016.1261049.

[26] T. K. Upadhyaya, A. Desai, and R. H. Patel, "Design of printed monopole antenna for wireless energy meter and smart applications," *Prog. Electromag. Letters*, vol. 77, pp. 27–33, Jun. 2018, doi: 10.2528/PIERL18042203.

[27] H. B. Chu and H. Shirai, "A compact metamaterial quad-band antenna based on asymmetric E-CRLH unit cells," *PIER C*, vol. 81, pp. 171–179, Feb. 2018, doi: 10.2528/PIERC17111605.

[28] U. Patel and T. K. Upadhyaya, "Design and analysis of compact μ-negative material loaded wideband electrically compact antenna for WLAN/WiMAX applications," *Prog. Electromag. M*, vol. 79, pp. 11–22, Feb. 2019, doi: 10.2528/PIERM18121502.

[29] C.-Y. Shuai and G.-M. Wang, "A Novel Planar Printed Dual-Band Magneto-Electric Dipole Antenna," *IEEE Access*, vol. 5, pp. 10062–10067, Jun. 2017, doi: 10.1109/ACCESS.2017.2712616.